ELSEVIER

Polymer 43 (2002) 7051–7061

polymer

www.elsevier.com/locate/polymer

Polymer Communication

Synthesis and mesomorphic properties of poly(oxyethylene)s containing alkylsulfonylmethyl or alkylthiomethyl side groups

J.-C. Lee[a,*], M.-Y. Lim[a], K. Oh[a], Y.G. Kim[a], H.B. Lee[a], S.-Y. Park[b], B.L. Farmer[c]

[a]*School of Chemical Engineering, Seoul National University, Seoul 151-744, South Korea*
[b]*Department of Polymer Science, Kyungpook University, Daegu 702-701, South Korea*
[c]*Air Force Research Laboratory, Materials and Manufacturing Directorate, Wright-Patterson Air Force Base, OH 45433-7750, USA*

Received 7 June 2002; received in revised form 4 September 2002; accepted 4 September 2002

Abstract

(*n*-Hexadecylsulfonyl)methyl-substituted poly(oxyethylene) (16SP), (*n*-hexadecylthio)methyl-substituted poly(oxyethylene) (16TP), [(6-*n*-nonylsulfonyl)hexylthio]methyl-substituted poly(oxyethylene) (9S6TP), and [(6-*n*-nonylsulfonyl)hexylsulfonyl]methyl-substituted poly(oxyethylene) (9S6SP) were synthesized. 9S6SP and 16SP containing sulfonylmethyl side groups showed highly ordered smectic layer structures at room temperature and liquid crystalline behavior at higher temperatures, while 9S6TP and 16TP containing thiomethyl side groups did not show any liquid crystalline behavior. The ordered phases of the polymers were studied using differential scanning calorimetry, cross-polarizing optical microscopy, and X-ray diffraction. The unusual liquid crystallinity of 16SP and 9S6SP was ascribed to the amphiphilic character of these polymers.

Keywords: Liquid crystalline polymer; Side chain crystallization; Poly(oxyethylene)

1. Introduction

It is well known that polymers with long alkyl side chains show liquid crystalline phases and/or side chain crystallization behavior. Many rigid rod polymers such as polyisocyanates, aromatic polyesters, aromatic polyamides, and polypeptides containing the flexible alkyl side chains show thermotropic liquid crystalline (LC) phases when the number of carbon atoms in the side group is within a certain range [1–14]. For example the polyisocyanates with side chain length of $4 \leq n \leq 13$ carbon atoms and the aromatic polymers with $n \leq 13$ show thermotropic LC phases [15,16]. When n is 13 or higher, crystalline phases were observed due to the side chain crystallization. Flexible backbone polymers with long alkyl side chains ($n > 10$) such as poly(*n*-alkyl acrylate)s, poly(*n*-alkyl methacrylate)s, and aliphatic polyester derivatives always show the side chain crystallization behavior, while these polymers with shorter side chains are always amorphous [17–24]. The liquid crystalline phases of such polymers were obtained only when anisotropic rod-like or disk-like mesogens were incorporated into side chains with flexible spacers between the backbone and the mesogenic unit [25–27]. Recently Lee et al. synthesized poly(oxyethylene)s with *n*-octylthiomethyl side groups or *n*-octylsulfonylmethyl side groups [28]. Although these polymers have very flexible oxyethylene backbones and relatively short side chains, and they showed ordered phases. Poly(oxyethylene)s with *n*-octylsulfonylmethyl side groups were found to have smectic A liquid crystalline phases. However, the ordered phase of poly(oxyethylene)s with *n*-octylthiomethyl side groups could not be determined because the isotropic temperature of the polymer was very low, below −30 °C. The ordered behavior of these polymers was ascribed to the strong dipole–dipole interaction between the sulfone groups and/or the side chain ordering of the alkyl groups, while clear conclusion could not be made. Recently we also reported on the X-ray results of poly(oxyethylene)s with different side chain lengths such as [(6-*n*-alkylsulfonyl)hexylthio]methyl groups or [(6-*n*-alkylsulfonyl)hexylsulfonyl]methyl groups (alkyl = pentyl, heptyl, and nonyl) [29], where we described the structures of the polymers in detail.

To get a better understanding of this unusual ordered behavior of the polymers, as a continuous work we synthesized poly(oxyethylene)s containing longer side

* Corresponding author. Tel.: +82-2-880-7070; fax: +82-2-888-1604.
E-mail address: jongchan@snu.ac.kr (J.-C. Lee).

0032-3861/02/$ - see front matter
PII: S0032-3861(02)00626-2

chains with almost identical lengths such as [(6-*n*-nonylsulfonyl)hexylthio]methyl groups, [(6-*n*-nonylsulfonyl)hexylsulfonyl]methyl groups, (*n*-hexadecylthio)methyl groups, or (*n*-hexadecylsulfonyl)methyl groups. We intentionally synthesized these four polymers because: (1) The longer side chains can induce higher isotropic temperatures, then the structures can be determined easily. (2) Since the lengths of the side chains are identical, the differences of the ordered phases of these polymers are not due to the side chain length but due to the position and the concentration of the sulfone and thioether groups in the side chains. In this paper, we describe the synthesis of the polymers including the poly(oxyethylene)s containing [(6-*n*-nonylsulfonyl)-hexylthio]methyl groups or [(6-*n*-nonylsulfonyl)hexyl-sulfonyl]methyl groups because the synthetic procedure of these two polymers was not mentioned in Ref. [29] and compare the thermal behavior and ordered phases of the four polymers containing almost identical side chain lengths.

2. Experimental section

2.1. Materials

Poly[oxy(chloromethyl)ethylene] (Hydrin H®, Zeon Chemical Inc.) (PECH) was used as received. Methylene chloride and chloroform were refluxed over calcium hydride, and freshly distilled under nitrogen before each use. *N*,*N*-Dimethylacetamide (DMAc) was dried over molecular sieves (4 Å). Ethanol was distilled from magnesium, after refluxing under nitrogen. All other reagents and solvents were used as received.

2.2. Synthesis

2.2.1. Synthesis of (n-hexadecylthio)methyl-substituted poly(oxyethylene) (16TP)

Sodium *n*-hexadecanethiolate was prepared by adding hexadecanethiol to a solution of sodium ethoxide in ethanol; the solid residue obtained after evaporation of the solvent was washed with ether, filtered and dried under vacuum.

PECH (1.70 g, 18 mmol) was dissolved in 100 ml of DMAc, and sodium *n*-hexadecylthiolate (9.07 g, 32.4 mmol) were added. The reaction mixtures were magnetically stirred at 60 °C for 0.5 h and then poured into distilled water. The precipitate was further purified by several precipitations from THF solution into distilled water, and then dried under vacuum at 80 °C overnight. ^{1}H NMR ($CDCl_3$): δ 0.86 (t, 3H, $J = 6.9$ Hz, $-CH_3$), 1.02–1.43 (m, 26H, $S-CH_2-CH_2-(CH_2)_{13}-CH_3$), 1.43–1.81 (m, 2H, $S-CH_2-CH_2-(CH_2)_{13}-CH_3$), 2.52 (t, 2H, $J = 7.3$ Hz, $S-CH_2-CH_2-(CH_2)_{13}-CH_3$), 2.58–2.83 (m, 2H, $CH_2-S-CH_2-CH_2-(CH_2)_{13}-CH_3$), 3.48–3.83 (m, 3H, $O-CH_2-CH-$). The degree of conversion was calculated by comparing the triplet at 0.86 ppm (3H) with the backbone peak at 3.48–3.83 ppm (3H) that included the contribution of residual CE and was found to be almost 100%. 16TP was obtained in 90% yield.

2.2.2. Synthesis of (n-hexadecylsulfonyl)methyl-substituted poly(oxyethylene) (16SP)

1.00 g of 16TP was dissolved in 30 ml $CHCl_3$ at room temperature and the solution was cooled to 0 °C. A slight excess over two equivalents of *m*-chloroperoxybenzoic acid (*m*-CPBA) was added to the reaction solution. The reaction mixture was stirred for 1 h and then poured into methanol. The precipitated polymer was purified by several reprecipitations from chloroform solution into methanol until all *m*-CPBA and *m*-chlorobenzoic acid were removed. ^{1}H NMR ($CDCl_3$): δ 0.86 (t, 3H, $J = 6.9$ Hz, $-CH_3$), 1.05–1.59 (m, 26H, $SO_2-CH_2-CH_2-(CH_2)_{13}-CH_3$), 1.61–1.96 (m, 2H, $SO_2-CH_2-CH_2-(CH_2)_{13}-CH_3$), 2.78–3.11 (m, 2H, $SO_2-CH_2-CH_2-(CH_2)_{13}-CH_3$), 3.12–3.42 (m, 2H, $CH_2-SO_2-CH_2-CH_2-(CH_2)_5-CH_3$), 3.50–3.92 (m, 2H, $O-CH_2-CH-$), 3.93–4.22 (m, 1H, $-O-CH_2-CH-$). 16SP was obtained in 90% yield.

2.2.3. Synthesis of [(6-n-nonylsulfonyl)hexylthio]methyl-substituted poly(oxyethylene) (9S6TP)

*2.2.3.1. (6-n-Nonylthio)hexanol (**1**).* To a solution of sodium ethoxide (0.72 g, 10.5 mmol) in 20 ml ethanol was added 6-mercaptohexanol (1.34 g, 10 mmol). The mixture was stirred at room temperature for 20 min, and then 1-bromononane (2.28 g, 11 mmol) was added, and then stirred for 1 h. Hydrochloride aqueous solution (3 wt%, 20 ml) was added to the reaction mixture, and then the aqueous solution was extracted with chloroform. The organic layer was dried over magnesium sulfate. The solvent was removed to give 2.62 g (10 mmol, quantitative) of colorless oil. ^{1}H NMR ($CDCl_3$): δ 0.88 (t, 3H, $J = 6.78$, $-CH_3$), 1.22–1.62 (m, 23H, $CH_3-(CH_2)_7-CH_2-S-CH_2-(CH_2)_4-CH_2-OH$), 2.50 (m, 4H, $-CH_2-S-CH_2-$), 3.65 (t, 2H, $J = 6.60$, $-CH_2-OH$).

*2.2.3.2. (6-n-Nonylsulfonyl)hexanol (**2**).* To a stirred solution of **1** (2.62 g, 10 mmol) in methylene chloride was added *m*-CPBA (5.42 g, 22 mmol) for 1 h at room temperature. The reaction mixture was washed with 10% aqueous ammonia. The organic layer was dried over magnesium sulfate and the solvent was removed. The residue was purified by column chromatography (SiO_2, ethyl acetate/*n*-hexane = 1/2) affording 2.60 g (8.9 mmol, 89% yield) of a white solid sulfonylalcohol **2**. ^{1}H NMR ($CDCl_3$): δ 0.88 (t, 3H, $J = 6.96$, $-CH_3$), 1.27–1.63 (m, 19H, $CH_3-(CH_2)_6-CH_2-CH_2-SO_2-CH_2-CH_2-(CH_2)_3-CH_2-OH$), 1.85 (m, 4H, $-CH_2-CH_2-SO_2-CH_2-CH_2-$), 2.95 (m, 4H, $-CH_2-SO_2-CH_2-$), 3.65 (t, 2H, $J = 6.42$, $-CH_2-OH$).

*2.2.3.3. Methyl (6-n-nonylsulfonyl)hexane sulfonate (**3**).* Into a solution of **2** (2.60 g, 8.9 mmol) and methanesulfonyl

chloride (1.15 g, 9.9 mmol) in CH_2Cl_2 (20 ml) was added triethylamine (1.08 g, 10.7 mmol). The reaction mixture was stirred at room temperature for 1 h, and then was washed two times with 20 ml of hydrochloride 3 wt% aqueous solution. The organic layer was dried over magnesium sulfate. The solvent was removed to give 3.28 g (8.9 mmol) of pale yellow oil, which was used at the next step without purification.

*2.2.3.4. (6-n-Nonylsulfonyl)hexyl thioacetate (**4**).* To a stirred solution of **3** (3.28 g, 8.9 mmol) and thiolacetic acid (0.88 g, 11.6 mmol) in $CHCl_3$ was added triethylamine (1.35 g, 13.4 mmol). The reaction mixture was refluxed for 3 h. It was then washed two times with 20 ml of hydrochloride 3 wt% aqueous solution. The organic layer dried over anhydrous magnesium sulfate and the solvent was removed. Chromatography (SiO_2, ethyl acetate/*n*-hexane = 1/2) of the resulting residue afforded 2.8 g (8.0 mmol, 90%) of **4**. ^{1}H NMR ($CDCl_3$): δ 0.88 (t, 3H, $J = 6.78$, $-CH_3$), 1.20–1.60 (m, 18H, $CH_3-(CH_2)_6-CH_2-CH_2-SO_2-CH_2-CH_2-(CH_2)_3-CH_2-S-CO-CH_3$), 1.83 (m, 4H, $-CH_2-CH_2-SO_2-CH_2-CH_2-$), 2.33 (s, 3H, $-S-CO-CH_3$), 2.86 (t, 2H, $J = 7.15$, $-CH_2-S-CO-CH_3$), 2.94 (m, 4H, $-CH_2-SO_2-CH_2-$).

2.2.3.5. Synthesis of 9S6TP. To a stirred solution of sodium ethoxide (4.3 mmol) in ethanol (10 ml) was added **4** (1.50 g, 4.28 mmol). After stirring at room temperature for 20 min, the reaction mixture was transferred into a solution of poly[oxy(chloromethyl)ethylene] (0.26 g, 2.8 mmol) (PECH) in DMAc (40 ml). The reaction mixture was stirred at 60 °C for 1 h and then poured into distilled water. The precipitate was further purified by several precipitations from $CHCl_3$ into methanol and then dried under high vacuum at 60 °C overnight. This product was obtained in 92% yield. ^{1}H NMR ($CDCl_3$): δ 0.88 (t, 3H, $J = 6.93$, $-CH_3$), 1.20–1.60 (m, 18H, $-CH_2-(CH_2)_3-CH_2-CH_2-SO_2-CH_2-CH_2-(CH_2)_6-CH_3$), 1.83 (m, 4H, $-CH_2-CH_2-SO_2-CH_2-CH_2-$), 2.56 (t, 2H, $J = 6.94$, $-O-CH_2-CH-CH_2-S-CH_2-$), 2.60–2.85 (m, 2H, $-O-CH_2-CH-CH_2-S-CH_2-$), 2.95 (m, 4H, $-CH_2-SO_2-CH_2-$), 3.48 –3.85 (m, 3H, $-O-CH_2-CH-$).

2.2.4. Synthesis of ((6-n-nonylsulfonyl)hexylsulfonyl)-methyl-substituted poly(oxyethylene) (9S6SP)

To a stirred solution of 9S6TP (0.72 g, 1.9 mmol) in chloroform (20 ml) was added *m*-CPBA (1.17 g, 4.75 mmol). After stirring at room temperature for 1 h, the reaction mixture was poured into methanol, and the precipitate was purified by several reprecipitations from chloroform solution into methanol until all *m*-CPBA and *m*-chlorobenzoic acid were removed. The polymer was dried under vacuum at 120 °C for over night. The yield was 90%. ^{1}H NMR ($CDCl_3$): δ 0.88 (t, 3H, $J = 6.60$, $-CH_3$), 1.20–1.60 (m, 18H, $-CH_2-(CH_2)_3-CH_2-CH_2-SO_2-CH_2-CH_2-(CH_2)_6-CH_3$), 1.83 (m, 4H, $-CH_2-CH_2-SO_2-CH_2-CH_2-(CH_2)_6-CH_3$), 2.85–3.20 (m, 6H, $-SO_2-CH_2-(CH_2)_3-CH_2-CH_2-SO_2-CH_2-$), 3.30 (br, 2H, $-O-CH_2-CH-CH_2-SO_2-$), 3.55–3.95 (m, 2H, $J = 7.15$, $-O-CH_2-CH-$), 4.08 (br, 1H, $-O-CH_2-CH-$).

2.3. Methods

^{1}H NMR spectra were obtained on 300 MHz (JEOL JNM-LA 300) using $CDCl_3$ as solvent.

Differential scanning calorimetry (DSC) was carried out on a TA DSC-2010. The heating and cooling rates were from 1 to 10 °C/min and the transition temperatures were given at the maxima or minima of the endothermic peaks. Pure Indium was used to calibrate the instrument.

Thermal gravimetric analysis (TGA) was carried out on a TA TGA-2050. Heating rate was 10 °C/min.

Cross-polarizing optical microscopy of the polymer samples, which sandwiched between two glass slide, was performed on a Nikon polarizing optical microscope equipped with a Mettler FP-82 hot-stage controlled by Mettler FP-800 central processor. The magnification was 400 ×.

Wide-angle X-ray diffraction patterns were recorded on both Kodak Direct Exposure film and a phosphor image plate (Molecular Dynamics) in a Statton camera. Monochromatic Cu K_α radiation from a rotating anode X-ray generator operating at 40 kV and 240 mA was used. The sample to film distance was calibrated using SiO_2 powder. X-ray patterns at high temperatures were obtained using a heating accessory for the Statton camera.

Synchrotron wide-angle X-ray scattering for some powder samples (16SE, 9S6TP) was conducted using the 3C2 beam line at the Pohang Light Source, Korea. Fiber specimens for X-ray study were prepared by drawing (with tweezers) the isotropic melt on a slide glass. Powder samples were prepared by filling the powder into glass capillaries. The glass capillaries were heated above the isotropic temperatures of the polymers, then cooled down to room temperature before the X-ray experiments to remove any annealing effects and to make homogeneous bulk samples. Higher temperature patterns from Statton camera and synchrotron source were obtained using the homogeneous bulk samples upon heating. The X-ray pattern was obtained at a constant temperature by equilibrating the sample chamber at a desired temperature. Therefore we believe that the high temperature X-ray patterns indicate the equilibrium structures.

3. Results and discussion

The synthetic routes and the chemical structures of 16TP, 16SP, 9S6TP, and 9S6SP are shown in Scheme 1. 16TP was made by the reaction of PECH and sodium hexadecanethiolate. Previously, when poly(oxyethylene)s containing

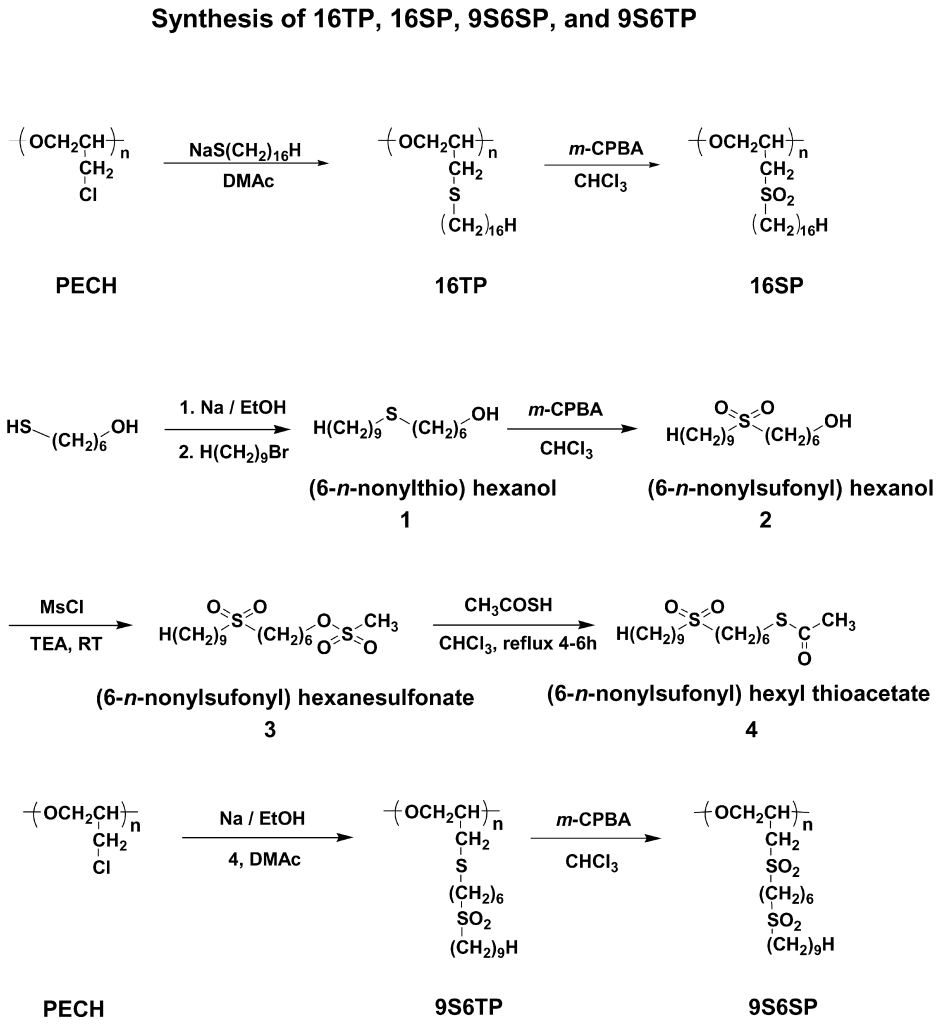

Scheme 1.

shorter alkylthio side chains were synthesized, 100% conversion was obtained using 180 mol% of sodium alkanethiolate at room temperature without any polymer precipitation [30]. This time using the same reaction condition the polymer precipitated within 1 min and the conversion was only 50%. The conversion increased with the increase of the reaction temperature; still polymer precipitation was observed. When the reaction temperature was above 100 °C, the resultant polymer was not soluble in any solvent. Probably radicals that can be generated easily by the cleavage of the weak C–S linkage in the side chain at high temperature cross-linked the polymer chains. When lower polarity solvents such as $CHCl_3$ and THF were employed, no precipitation was observed during the reaction, but conversions were very low. 100% conversion of PECH to solvent-soluble 16TP was obtained using sodium *n*-hexadecanethiolate at 60 °C. 16SP was obtained by oxidation of 16TP using *m*-CPBA. In the previous papers, the oxidation of thiolate polymers with shorter side chains was discussed in detail [28,30]. The structures of 16TP and 16SP were confirmed by ^{1}H NMR spectra. The number average molecular weight (M_n) and polydispersity index of 16TP were 47,200 and 2.1, respectively, and those of 16SP were 22,000 and 2.9, respectively. **2** was obtained in high yield from oxidation of **1** using *m*-CPBA, which was obtained by alkylation of 6-mercaptohexanol. Mesylation of **2** followed by a substitution reaction using thiolacetic acid yielded **4**. 9S6TP was made by reaction of PECH and **4** with sodium ethoxide in DMAc. The sodium ethoxide was prepared by adding sodium into dry ethanol under nitrogen atmosphere before use. 9S6SP was obtained by oxidation of 9S6TP using *m*-CPBA. Almost 100% conversions of PECH to 9S6TP and 9S6TP to 9S6SP were observed from ^{1}H NMR (Fig. 1). The number average molecular weight (M_n) and polydispersity index of 9S6TP were 67,000 and 3.1, respectively, and those of 9S6SP were 30,000 and 2.6, respectively. M_n of the starting polymer, PECH, was 390,000. There might be some chain cleavage during the reaction. Since polystyrene standards were used in the calculation of the molecular weight and the distribution, the extent of the cleavage is not certain. As we were interested in the side-chain ordered phases of poly(oxyethylene)

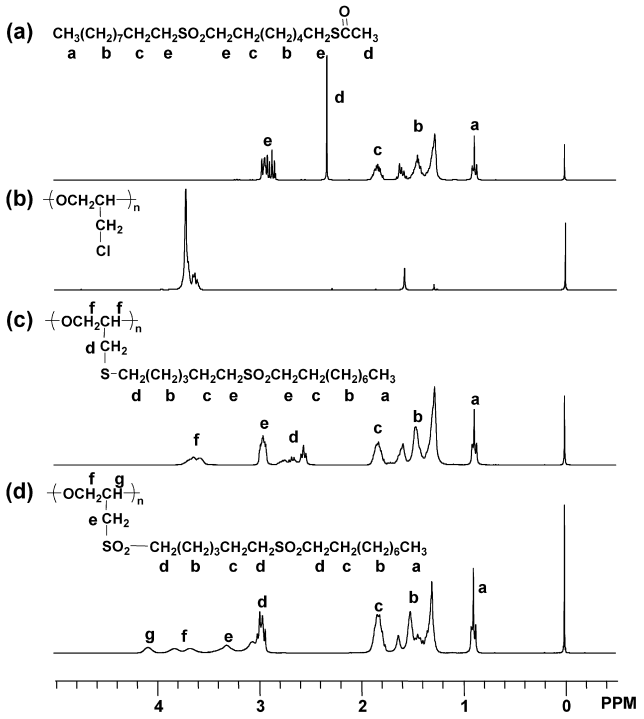

Fig. 1. ^{1}H NMR spectra of (a) (6-nonylsulfonyl)hexyl thioacetate, (b) PECH, (c) 9S6TP, and (d) 9S6SP.

derivatives, we intentionally chose the PECH (Hydrin H®) as the starting polymer since it is amorphous. Therefore, ordered properties discussed in the following part of the papers are thoroughly due to the side chains.

Fig. 2 shows the DSC cooling and heating curves of 16TP and 16SP at different scan rates of 1, 3, 5, and 10, respectively. 16TP has three endotherms upon 1 °C/min heating scan at 29.1 °C ($\Delta H = 23.6$ J/g), 39.7 °C ($\Delta H = 25.4$ J/g), 56.1 °C ($\Delta H = 31.4$ J/g), and also three exotherms at 50.3 °C ($\Delta H = 34.5$ J/g), 34.6 °C ($\Delta H = 24.3$ J/g), 25.6 °C ($\Delta H = 16.5$ J/g) upon the cooling scan of 1 °C/min. 16SP has three endotherms upon 1 °C/min heating scan at 60.1 °C ($\Delta H = 7.0$ J/g), 93.7 °C ($\Delta H = 13.7$ J/g), and 158.1 °C ($\Delta H = 1.2$ J/g), and also three exotherms at 156.9 °C ($\Delta H = 1.1$ J/g), 93.0 °C ($\Delta H = 13.2$ J/g), and 50.0 °C ($\Delta H = 5.2$ J/g) upon the cooling scan of 1 °C/min. The DSC results of 9S6TP and 9S6SP from 1 °C/min scan rates are listed in Table 1. The highest transition temperatures of the polymers were

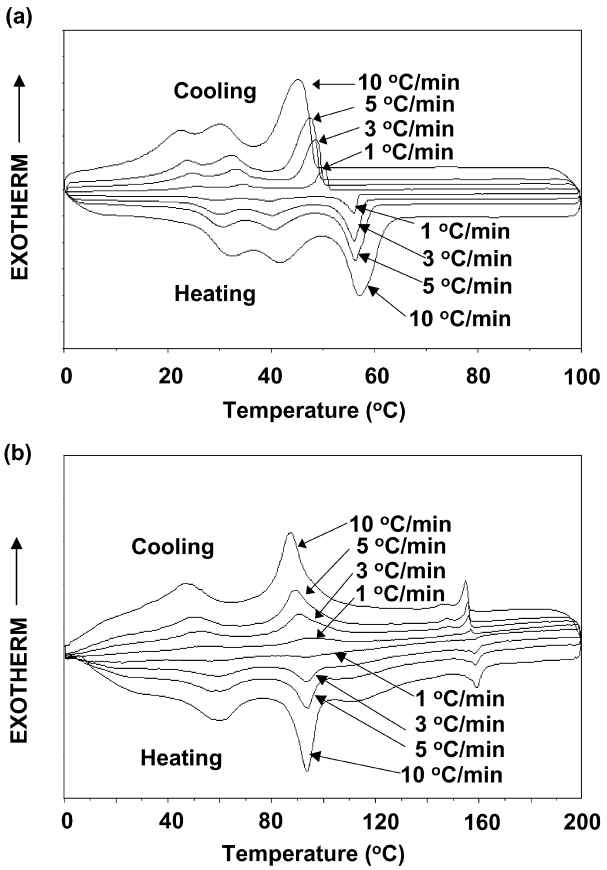

Fig. 2. DSC curves of (a) 16TP and (b) 16SP.

defined as the isotropic temperatures (T_i). Because below these temperatures ordered structures were observed from X-ray and POM studies. Above T_i wide-angle reflections changed to amorphous halo. These results are shown in the later part of this paper. T_is of 16TP obtained from the heating scans of 1, 3, 5, and 10 °C/min were 56.1, 56.1, 56.3, 57.2 °C, respectively, and those from the cooling scans of 1, 3, 5, and 10 °C/min were 50.3, 48.7, 47.5, and 45.2 °C, respectively. Using these values equilibrium T_is were obtained by extrapolation of linear plots of T_i versus heating/cooling rate to 0 °C/min heating/cooling rate and they were 55.8 and 50.5 °C for heating and cooling rates, respectively; the detailed procedure for the calculation of the equilibrium transition temperatures can be found elsewhere [31,32]. Therefore the supercooling of 16TP at

Table 1
DSC results of the polymers

	Second heating endotherms, °C (ΔH, J/g)	First cooling exotherm, °C (ΔH, J/g)
16TP	29.1 (23.6), 39.7 (25.4), 56.1 (31.4)	50.3 (34.5), 34.6 (24.3), 25.6 (16.5)
16SP	60.1 (7.0), 93.7 (13.7), 158.1 (1.2)	156.9 (1.1), 93.0 (13.2), 50.0 (5.2)
9S6TP	72.2 (4.0), 98.7 (36.5)	95.2 (32.3), 76.7 (11.5), 57.7 (10.8)
9S6SP	145.5 (17.7), 165.9 (8.0)	135.8 (21.8), 165.3 (8.0)

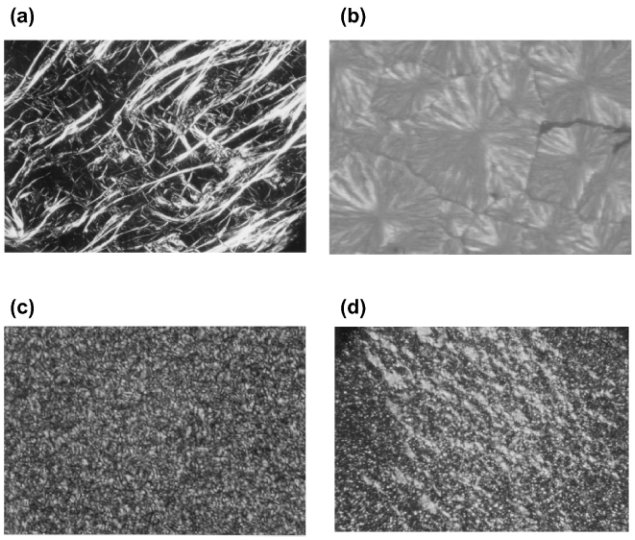

Fig. 3. Cross-polarizing optical microscopic photographs for (a) 16TP at 50 °C, (b) 9S6TP at 90 °C, (c) 16SP at 120 °C, and (d) 9S6SP at 160 °C.

equilibrium state is about 5.3 °C. This non-zero value of supercooling indicates that possibly the ordered phase formation at T_i upon cooling includes nucleation and growth. The enthalpy changes of the 16TP at T_is obtained from 1 °C/min heating and cooling scans were about 31.4 and 34.3 J/g, respectively. The non-zero value of the supercooling and the relatively large values of enthalpy changes indicate that 16TP has a highly ordered phase below T_i and this phase should not be liquid crystalline. T_is of 16SP obtained from the heating scans of 1, 3, 5, and 10 °C/min were 157.8, 158.7, 158.9 and 159.5 °C, respectively, and those from the cooling scans were 156.9, 156.0, 155.6, and 155.0 °C, respectively. Therefore the supercooling at equilibrium T_i of 16SP is almost 0 °C indicating a reversible phase transition. The enthalpy changes of the T_is for 16SP obtained from the 1 °C/min heating and cooling scans were about 1.2 and 1.1 J/g, respectively. The zero supercooling and the very small values of enthalpy changes are the strong indication of liquid crystallinity of 16SP below the T_i [33,34]. The supercoolings for 9S6TP and 9S6SP were also calculated and found to be 3.6 and 0.0 °C, respectively. The enthalpy changes at T_is for 9S6TP and 9S6SP were about 36.5 and 8.0 J/g, respectively. Using the same rationale we could postulate that 9S6TP and 9S6SP have a highly ordered phase (crystal or condis crystal) and a liquid crystalline phase below their T_is, respectively.

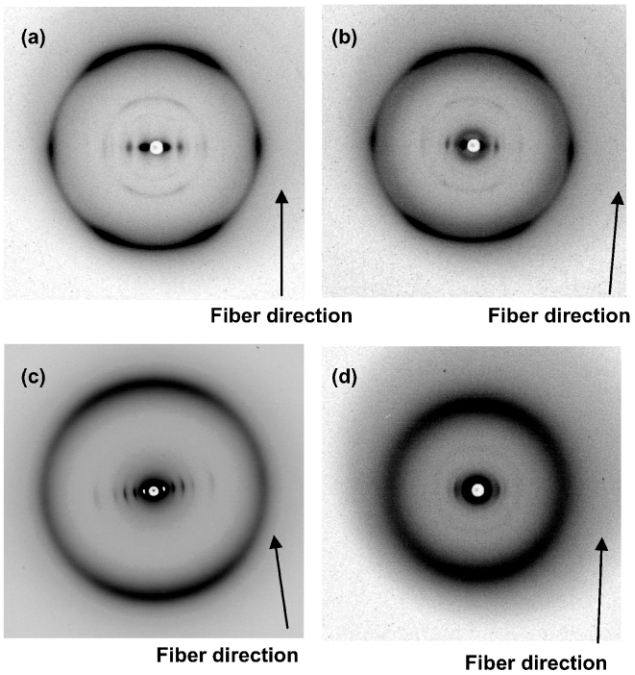

Fig. 4. X-ray patterns of drawn fiber of (a) 16TP at 25 °C, (b) 16TP at 45 °C, (C) 16SP at 25 °C, and (d) 16SP at 125 °C.

From cross polarizing optical microscopy observation, ordered phases of the polymers were also investigated. Fig. 3a shows a thread-like texture of 16TP at 45 °C. Small and very thin birefringent threads start to appear from 51 °C upon cooling the isotropic melt at a cooling rate of 3 °C/min. Within a few minutes, the threads became more birefringent and thicker, and also more threads appeared. When 9S6TP was cooled from the isotropic melt, very small points started to appear from the melt from about 95 °C, and within a few minutes they turned into typical spherulites and then impinged on each other. The spherulite texture observed at 90 °C is shown in Fig. 3b. This result indicates that the formation of ordered phases from isotropic melts of 16TP and 9S6TP involves the nucleation and growth resulting in non-zero supercooling values. However, both 16SP and 9S6SP (Fig. 3c and d) showed grainy textures and the nucleation and growth procedure was not observed. It is well known that high viscosity polymer melts can prevent the formation of normal liquid crystalline texture [35]. This is especially true for smectic liquid crystalline polymers; frequently, a grainy texture of birefringent domains is seen. Therefore it is probable that 16SP and 9S6SP have smectic liquid crystalline phases below their T_is. We could not observe glass transition temperatures of these polymers, even from heating scans after quenching the polymer melt in the DSC cell. The ordered structures of the polymers are further studied using X-ray diffraction.

Fig. 4 shows X-ray patterns of the drawn fibers of 16TP and 16SP. At room temperature 16TP shows a highly ordered hexagonal packing of the side alkyl chains, which can be clearly identified by the six wide-angle reflections on the equator and 60° from the equator in the outer rings at $d = 4.14$ and 8.27 Å, respectively. This X-ray pattern is typical for most comb-like vinyl polymers [36]. The d-spacing value, 4.14 Å, is slightly smaller than or close to the typical hexagonal d-spacing value of 4.17–4.20 Å for the comb-like vinyl polymers with long alkyl side chains [17, 36] and almost identical with the d-spacing value, 4.13 Å, of atactic poly[oxy(octadecyl)ethylene] reported by Magagnini et al. [37]. Therefore 16TP has a typical hexagonal

Table 2
The *d*-spacings of 16TP at different temperatures

Temperature (°C)	*d*-Spacing (Å)				
25	50.4	16.4	12.4	8.27	4.14
35	50.1	16.2	12.4	8.38	4.19
40	49.8	16.2	12.3	8.40	4.21
45	49.1	16.2	12.3	8.46	4.23
50	48.2	16.0	12.0	8.48	4.24
55	47.3	15.6		8.62	4.31

packing of the side chains. A series of reflections along the equator at $d = 50.4$, 16.4 and 12.4 Å corresponding to 001, 003, and 004 indices of periodic layer indicates that 16TP has a highly ordered layer structure. The 50.4 Å value is very close to the length that could be calculated from the assumption that the side chains are fully extended with trans conformations at the right angles on both sides of the polymer backbone. Therefore 16TP has a double layer structure. The fiber X-ray patterns of 16TP were also obtained at 35, 40, 45, and 50 °C, respectively, and they were almost identical, although the *d*-spacing of the small-angle reflection decreases and that of the wide angle reflection increases slightly with increasing temperature (Table 2). Fig. 4b shows the X-ray pattern obtained at 45 °C. Therefore the ordered structure of 16TP at room temperature little changed up to T_i. Above 50 °C the sharp wide-angle reflection changes to amorphous halo as shown in Fig. 5, indicating that the side chain crystal melts. The ordered structure and the thermal behavior of 16TP are almost identical with those of atactic poly[oxy(octadecyl)ethylene] [37]. The two polymers have almost

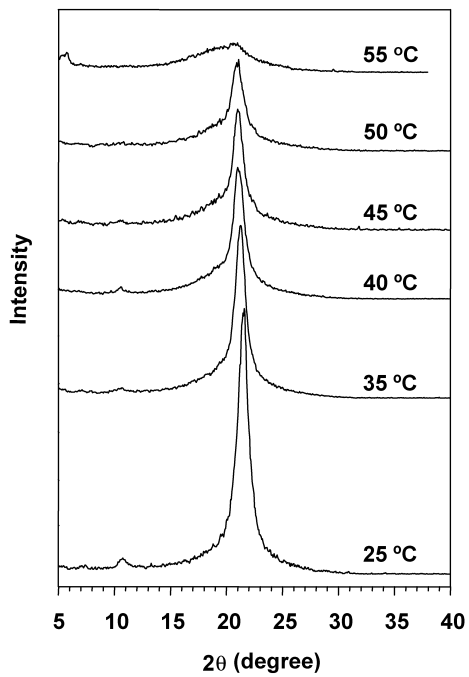

Fig. 5. Wide-angle powder X-ray patterns of 16TP at different temperatures.

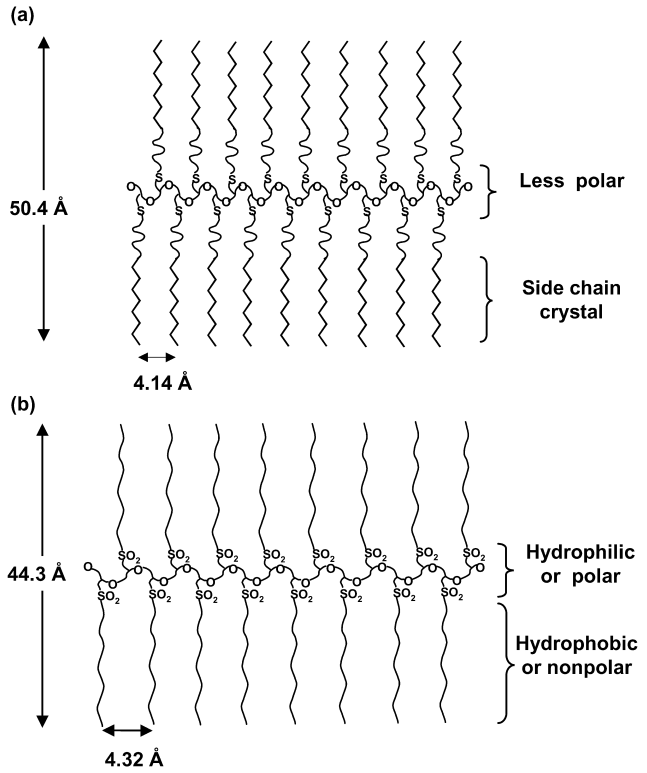

Fig. 6. Schematic diagram of (a) 16TP and (b) 16SP.

identical chemical structures; the only difference between the two is that the side chain of atactic poly[oxy(octadecyl)ethylene] is composed of all methylene groups, while that of 16TP contains one thioether group. This minor difference did not affect, if any, the properties of the polymers.

The number of crystallizing methylene groups in the side chain of 16TP was calculated on the basis of the values of heat of fusion, $\Delta H = 3.07$ kJ/mol CH_2, of *n*-alkanes in hexagonal packing [19,38]. The number for 16TP was found to be 8.24; since 16TP maintains its hexagonal structures below T_i, the average value ($\Delta H = 25.29$ kJ/mol) of the total enthalpy changes obtained from different heating rates of DSC scans was used for the calculation. Therefore about eight methylene groups in the outer part of the side chains participate in the side chain crystallization, while the other eight methylene groups in the inner part form amorphous state. Previously identical results were reported by Jordan et al., from their thermodynamic studies on the side chain crystallization of the comb-like vinyl polymers [18,19]. From these results a possible structure of 16TP was estimated and is represented in Fig. 6a.

16SP exhibits meridional arcs ($d = 4.32$ Å) in the wide-angle region at room temperature as shown in Fig. 4c. It is very unusual for such a comb-like polymer with hexadecyl side chains to have such a large *d*-spacing value of 4.32 Å. In general, polymers with long alkyl side chains ($n > 12$) including 16TP, comb-like vinyl polymers [26,39,40],

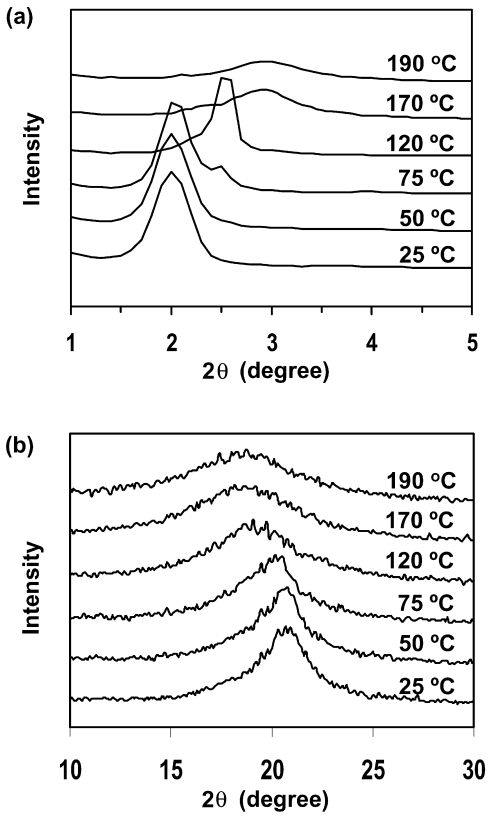

Fig. 7. Powder X-ray patterns of 16SP obtained from Pohang Synchrotron source at different temperatures: (a) small angle region; (b) wide angle region.

rigid-rod polymers [4–6,11,12,16,41], and amphiphilic polymers [42–44] exhibit hexagonal packings with one or more sharp wide-angle reflections at *d*-spacing values less than 4.2 Å. One possible explanation is that the bulky sulfone group separates the distance between the side chains resulting in the larger *d*-spacing value. However, poly-(acrylamide) containing alkyl phosphatidylcholine side groups [42] and poly(4-vinylpyridine)-pentadecylphenol [44] which have even bulkier groups in the side chains show the *d*-spacing values less than 4.2 Å. A series of reflections along the equator in the small-angle region implies that 16SP has a highly ordered layer structure. The *d*-spacing of small-angle primary reflection, 44.3 Å, is smaller than that of 16TP by 6 Å, indicating that the replacement of the thioether units in the side chains with the bulkier and very polar sulfone groups decreases the distance between the backbones in the double layer structure with increasing distance between the side chains. There are two possible explanation for the smaller values of the small-angle primary reflection of 16SP: (1) 16SP have a conformationally disordered crystalline structure (condis crystal) at room temperature; the backbone is atactic and the side chains are not fully extended (possibly some part of the side chain units might have gauche conformation) with highly ordered layer structure [45]. (2) The end parts of the side chains are interdigitated to form a interdigitating layer structure [46]. Fig. 4d shows the fiber X-ray pattern of 16SP at 125 °C which is between the isotropic and the second highest transition temperatures of the polymer. The wide-angle reflection becomes broader. In the small-angle region, there are still a series of reflections, although the number and the intensity of the peaks decrease, implying that still the layered structure is not totally destroyed. Above 160 °C wide-angle pattern becomes much broader (amorphous halo), while the major small-angle peak still remains, which will be further discussed using the powder X-ray results as follows.

Powder X-ray patterns from synchrotron source for 16SP at different temperatures are shown in Fig. 7. The powder patterns at room temperature and 50 °C are almost identical. At 75 °C (between the lowest transition and the second highest transition temperatures) a strong small-angle reflection at $d = 44.4$ Å with a small shoulder peak at $d = 35.6$ Å and a wide-angle reflection at $d = 4.41$ Å are observed. The wide-angle reflection might also have a shoulder at $d = 4.58$ Å, while it is not very clear with the resolution of our experiment. Therefore, there might be two different layer structures in this temperature region. Further detailed X-ray investigation is under progress to elucidate the structure of this polymer in this temperature region. At 120 °C (between the second highest transition temperature and the T_i) the small-angle reflection shifts to a higher angle without changing the peak width too much, while the wide-angle reflection moves to a lower angle accompanied by line broadening, indicating that the highly ordered layer structure becomes less ordered. The fiber X-ray pattern at this temperature is typical for a liquid crystalline smectic A phase (Fig. 4d). The X-ray diffraction curves at the isotropic state (170 and 190 °C) show a broad small-angle reflection at $d = 30.5$ Å and a broad wide-angle amorphous halo at $d = 4.92$ Å. In the isotropic state the intensity of the small-angle reflection is much higher than that of the wide-angle amorphous reflection that was confirmed from a full-scale spectrum. Such a small-angle reflection in the homogeneous melt state was observed from block copolymers and mesomorphic polymer-surfactant systems [47–50]. This might explain the driving force of the unusual liquid crystalline behavior of 16SP. The ordered phases of both the block copolymers and polymer–surfactant systems are due to the phase separations of two components with different polarities. Then, 16SP could be considered as an amphiphilic polymer composed of a polar (and/or hydrophilic) backbone part and a non-polar (and/or hydrophobic) alkyl tails as shown in Fig. 5b. Possibly the highly polar sulfone groups near to the oxyethylene backbone increase the polarity of the backbone part to induce a phase separation, which in turn generate a layered liquid crystalline phase between the second highest transition temperature and T_i. However, 16TP, which has less polar or non-polar thioether groups near to the backbone, does not have such a big polarity difference between the backbone and the side chain (Fig. 6a).

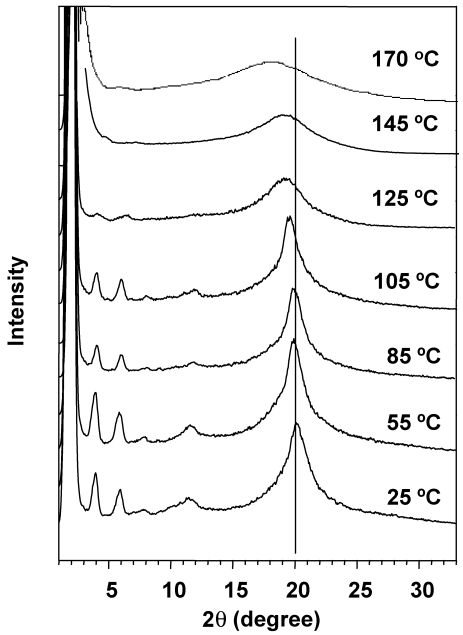

Fig. 8. Powder X-ray patterns of 9S6SP at different temperatures.

Since X-ray results of 9S6TP and 9S6SP are mentioned in a separate publication [29], only the results that are not mentioned and are related to the object of this paper will be discussed. 9S6TP showed a highly ordered layer structure at room temperature with a small-angle primary reflection at $d = 48.0$ Å and a wide-angle reflection at $d = 4.32$ Å. This highly ordered layer structure little changed up to T_i, although the d-spacing of the small-angle reflection decreases and that of the wide angle reflection increases slightly with increasing temperature; this behavior is similar to that of 16TP. 9S6SP showed also showed highly ordered layer structure with a primary small-angle reflection at $d = 46.1$ Å and a wide-angle reflection at $d = 4.47$ Å at room temperature, and showed a S_A liquid crystalline phase between the second highest transition temperature and T_i. This behavior is almost identical with that of 16SP. 9S6SP also exhibited a small-angle scattering peak above T_i as shown in Fig. 8. 9S6TP, which contains thiomethyl side groups, shows no obvious small-angle peak above its T_i. Therefore both 16SP and 9S6SP, which contain sulfonylmethyl side groups, exhibit liquid crystalline behavior and show the quite strong small-angle peaks probably corresponding to the characteristic block copolymer-like concentration fluctuation in the homogeneous melt state [49].

Table 3
Thermal stability of polymers by TGA

	$T_{d,0}$ [a] (°C)	$T_{d,1/2}$ [b] (°C)	Y [c] (%)
16TP	281	342	4.7
16SP	297	345	2.8
9S6TP	313	367	2.3
9S6SP	335	384	2.0

[a] Initial decomposition temperature.
[b] Half decomposition temperature.
[c] Char yield at 500 °C.

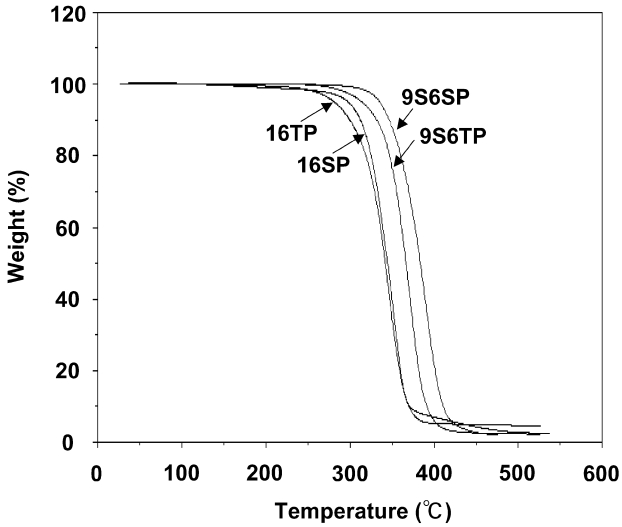

Fig. 9. TGA thermograms of the polymers under N_2.

Finally the thermal stability of the polymers was evaluated using dynamic thermogravic analysis (TGA) under N_2 (Table 3). 9S6SP containing two sulfone groups per a side chain shows the highest thermal stability, and 16TP having no sulfone groups shows lowest decomposition temperature. Furthermore, the sulfone group in the middle of the side chains increases the thermal stability because 9S6TP and 9S6SP have higher decomposition temperatures than 16TP and 16SP. Fig. 9 shows the decomposition behavior of the polymers.

Table 4 shows the summary of the properties for the polymers used in this study. The wide-angle d-spacing value at room temperature is 9S6SP > 16SP ≅ 9S6TP > 16TP, indicating the more the sulfone groups in the side chain, the larger the wide-angle d-spacing value of the polymer. The layer thickness at room temperature is 16TP > 9S6TP > 9 S6SP > 16SP indicating the poly(oxyethylene)s with thiomethyl side group have longer inter-backbone distance. The T_is are in the order of 9S6SP > 16SP > 9S6TP > 16TP. The T_i value of 9S6SP containing two sulfone groups in the side chain is higher than those of 16SP and 9S6TP, which contain one sulfone group in the side chain each, by 6.6 and 59.6 °C, respectively. Obviously the very polar and bulky sulfone group near to the backbone affects the transition temperature predominantly. 16SP and 9S6SP containing sulfonylmethyl side groups have almost no supercoolings and very small values of ΔHs, indicating that these polymers show reversible phase transition behavior between isotropic state and liquid crystalline phase. 16TP and 9S6TP containing thiomethyl side groups have relatively large values of the supercoolings and the ΔH, indicating that these polymers have higher ordered structures than the liquid crystalline 16SP and 9S6SP have. 16TP and 9S6TP show spherulitic and thread-like textures, respectively, and they were formed through nucleation and growth. The liquid

Table 4
Differential scanning calorimetry, cross-polarizing optical microscopy, and X-ray diffraction results of the polymers

	Wide-angle *d*-spacing (Å)	Layer thickness (Å)	Isotropic temperature[a] (°C)	Supercooling[b] (deg)	ΔH [c] (J/g)	POM texture
16TP	4.14[d]	50.4[d]	56.1	5.3	31.4	Thread-like
9S6TP	4.32[d]	48.0[d]	98.7	3.6	36.5	Spherulite
16SP	4.32[d], 4.60[e]	44.3[d], 35.3[e]	158.1	~0	1.2	Granule
9S6SP	4.47[d], 4.50[f]	46.1[d], 40.1[f]	165.9	~0	8.0	Granule

[a] Obtained from heating scan at 1 °C/min of DSC.
[b] Temperature difference between the isotropic temperatures at the equilibrium state obtained by extrapolating to zero heating and cooling rates, respectively.
[c] The enthalpy change of isotropic temperature obtained from heating scan at 1 °C/min of DSC.
[d] Obtained from powder X-ray pattern at room temperature.
[e] Obtained from powder X-ray pattern at 120 °C.
[f] Obtained from powder X-ray pattern at 145 °C.

crystalline 16SP and 9S6SP exhibit grainy textures from cross-polarizing optical microscopy experiments.

4. Conclusions

Four poly(oxyethylene)s containing long side chains with almost identical lengths (l6TP, 16SP, 9S6TP, and 9S6SP) were synthesized to investigate the effect of the sulfone groups on the ordered phases of the polymers. 16TP and 9S6TP composed of oxyethylene backbone and alkylthiomethyl side groups only showed highly ordered smectic crystals. 16SP and 9S6SP composed of oxyethylene backbone and alkylsulfonylmethyl side groups showed highly ordered layer structures at lower temperatures, and exhibited liquid crystalline behavior at higher temperatures. Therefore the sulfone groups near to the backbone induce the liquid crystalline phases of 16SP and 9S6SP; the liquid crystallinity of 16SP and 9S6SP is probably due the possible amphiphilicities of the polymers, because they are composed of the very polar sulfonyl-substituted oxyethylene backbone region and the non-polar long alkyl tail region. However, the sulfone groups in the middle of the backbone do not affect the overall structures of the poly(oxythylene)s. The small angle reflections observed above the isotropic temperatures from 16SP and 9S6SP might indicate the amphiphilic property of these polymers. Therefore we can presumably conclude that the liquid crystallinity of the poly(oxyethylene)s with *n*-octylsulfonylmethyl side groups is due to the amphiphilicity [28].

Acknowledgements

Financial support of this work by Korea Science and Engineering Foundation through Hyperstructured Organic Materials Research Center is gratefully acknowledged. Synchrotron X-ray experiments at PLS, Korea, were supported by POSCO, Korea. Soo-Young Park acknowledges financial support from Air Force Office of Scientific Research for an NRC postdoctoral Research Associateship.

References

[1] Aharoni SM. Macromolecules 1979;12:94.
[2] Watanabe J, Fukuda Y, Gehani R, Uematsu I. Macromolecules 1974; 17:1004.
[3] Herrmann-Schonherr O, Wendorff JH. Macromol Chem Rapid Commun 1986;7:791.
[4] Ballauff M. Macromol Chem Rapid Commun 1986;7:407.
[5] Ballauff M, Schmit GF. Mol Cryst Liq Cryst 1987;147:163.
[6] Rodriguez-Parada JM, Duran R, Wegner G. Macromolecules 1989; 22:2507.
[7] Ballauff M, Schmidt GM. Macromol Chem Rapid Commun 1987;8: 93.
[8] Stern R, Ballauf M, Lieser G, Wegner G. Polymer 1991;32:2096.
[9] Watanabe J, Takashina Y. Macromolecules 1991;24:3423.
[10] Clauss J, Schmidt-Rohr K, Adam A, Boeffel C, Spiess HW. Macromolecules 1992;25:5208.
[11] Červinka L. Polymer 1994;35:5225.
[12] Kim H, Park S-B, Jung JC, Zin W-C. Polymer 1996;13:2845.
[13] Watanabe J, Sekine N, Nematsu T, Sone M. Macromolecules 1996; 29:4816.
[14] Lauter U, Meyer WH, Enkelmann V, Wegner G. Macromol Chem Phys 1998;199:2129.
[15] Aharoni SM. J Polym Sci, Polym Phys Ed 1980;18:1303.
[16] Lee JL, Pearce EM, Kwei TK. Macromolecules 1997;30:6877.
[17] Inomata K, Sakamaki Y, Nose T, Sasaki S. Polym J 1996;28:986.
[18] Jordan EF, Artymyshyn B, Speca A, Wrigley AN. J Polym Sci, Part A 1971;9:3349.
[19] Jordan EF, Feldeisen DW, Wrigley AN. J Polym Sci, Part A 1971;9: 1835.
[20] Jordan EF. J Polym Sci, Part A 1971;9:3367.
[21] Andruzzi F, Hvilsted S, Paci M. Polymer 1994;35:4449.
[22] Magagnini PL, Tassi EL, Andruzzi F, Paci M. Polym Sci 1994;36: 1792.
[23] Gerum W, Höhne GWH, Wilke W. Macromol Chem Phys 1995;196: 3791.
[24] Russel KE, Mcfaddin DC, Hunter BK, Heyding RD. J Polym Sci, Polym Phys Ed 1996;34:2447.
[25] Percec V, Pugh C. In: McArdle CB, editor. Side chain liquid crystal polymers. New York: Blackie; 1989. p. 30–105.
[26] Shibaev VP, Freidzon YS, Kostromin SG. Liquid crystalline and mesomorphic polymers. New York: Springer; 1994. p. 77–148.
[27] Dubois J-C, Barny PL, Mauzac M, Noel C, Handbook of liquid crystals, vol. 3. New York: Wiley-VCH; 1998. p. 207–76.
[28] Lee J-C, Litt MH, Rogers CE. Macromolecules 1998;31:2440.
[29] Park S-Y, Farmer BL, Lee J-C. Polymer 2002;43:177.
[30] Lee J-C, Litt MH, Rogers CE. Macromolecules 1997;30:3776.
[31] Bershtein VA, Egorov VM. Differential scanning calorimetry of polymers. New York: Ellis Horwood; 1994. p. 134–41.

[32] Park S-Y, Zhang T, Interrante LV, Farmer BL. Macromolecules 2002; 35:2776.
[33] Noel C. In: Chapoy LL, editor. Recent advances in liquid crystalline polymers. London: Elsevier; 1985. p. 135–64.
[34] Chen W, Toda A, Moon I-K, Wunderlich B. J Polym Sci, Polym Phys Ed 1999;37:1539.
[35] Donald AM, Windle AH. Liquid crystalline polymers. Cambridge: Cambridge University Press; 1992. p. 159–62.
[36] Platé NA, Shibaev VP. J Polym Sci, Macromol Rev 1974;8:117.
[37] Andruzzi F, Lupinacci D, Magagnini PL. Macromolecules 1980;13: 15.
[38] Kunusada H, Yuki Y, Kondo S, Goto K, Oda S. Polym J 1992;24:239.
[39] Yuki Y, Kunisada H, Miyake Y. Polym J 1991;23:939.
[40] Yokota K, Kougo T, Hirabayashi T. Polym J 1983;15:891.
[41] Zheng W-Y, Levon K, Laakso J, Österholm J-E. Macromolecules 1994;27:7754.
[42] Chen T-M, Wang Y-F, Kitamura M, Nakawa T, Sakurai I. J Polym Sci, Polym Chem Ed 1996;34:1155.
[43] Takahashi T, Kimura T, Sakurai K. Polymer 1999;40:5939.
[44] Ruokolainen J, Brinke G, Ikkala O, Torkkeli M, Serimaa R. Macromolecules 1996;29:3409.
[45] Wunderlich B. Thermochim Acta 1999;37:340–1.
[46] Hsieh HWS, Post B, Morawetz H. J Polym Sci, Polym Phys Ed 1976; 14:1241.
[47] de Gennes P-G. Scaling concepts on polymer physics. Ithaca, NY: Cornell University Press; 1979.
[48] Hamley IW. The physics of block copolymers. New York: Oxford University Press; 1998. Chapter 2.
[49] Ruokolainen J, Torkkeli M, Serimaa R, Vahvaselka S, Saariaho M, Brinke G, Ikkala O. Macromolecules 1996;29:6621.
[50] Huh J, Ikkala O, Brinke G. Macromolecules 1997;30:1828.